

Supporting Information

A Synergistic Chemodynamic-Photodynamic-Photothermal Therapy Platform Based on Biodegradable Ce-doped MoO_x Nanoparticles

Danyang Li,^a Enna Ha,^{*a} Jingge Zhang,^a Luyang Wang^b and Junqing Hu^{*a,c}

^a College of Health Science and Environmental Engineering, Shenzhen Technology University, Shenzhen 518118, P. R. China.

^b College of New Materials and New Energies, Shenzhen Technology University, Shenzhen 518118, P. R. China

^c Shenzhen Bay Laboratory, Shenzhen, 518132, P. R. China

* Corresponding author E-mail address: haenna@sztu.edu.cn; hujunqing@sztu.edu.cn

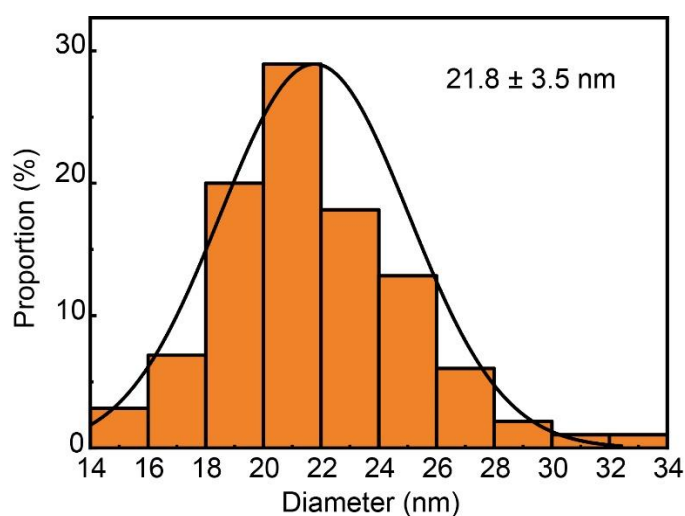


Figure S1. Size distribution profile of the CMO calculated from TEM.

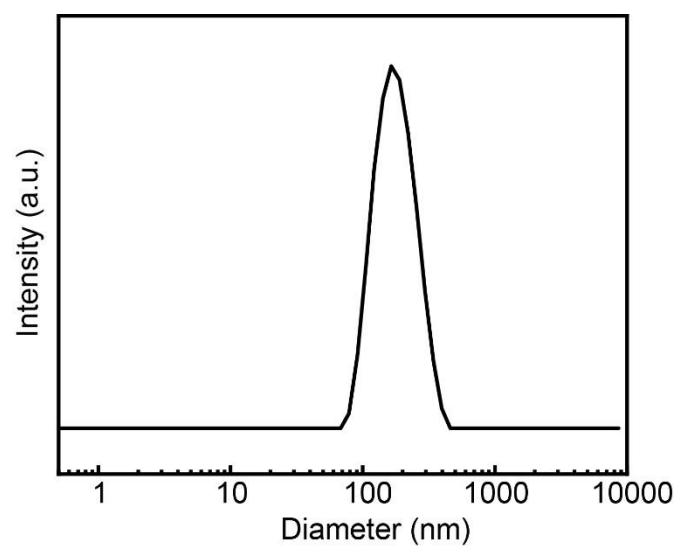


Figure S2. Dynamic light scattering diameter distribution of CMO in aqueous solution.

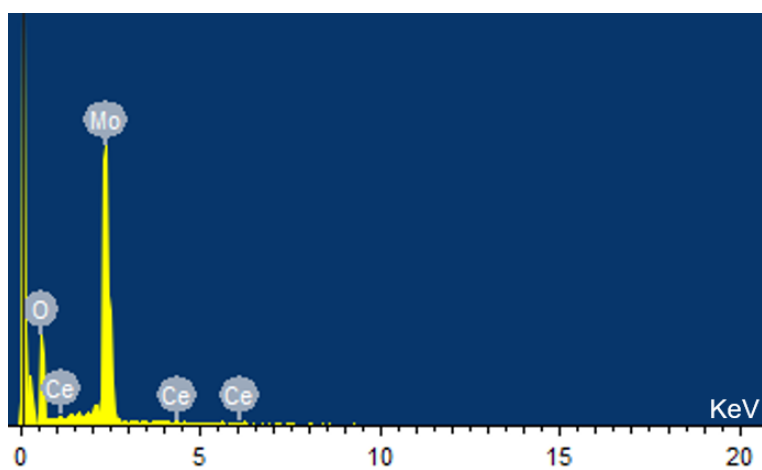


Figure S3. EDS spectrum of the CMO.

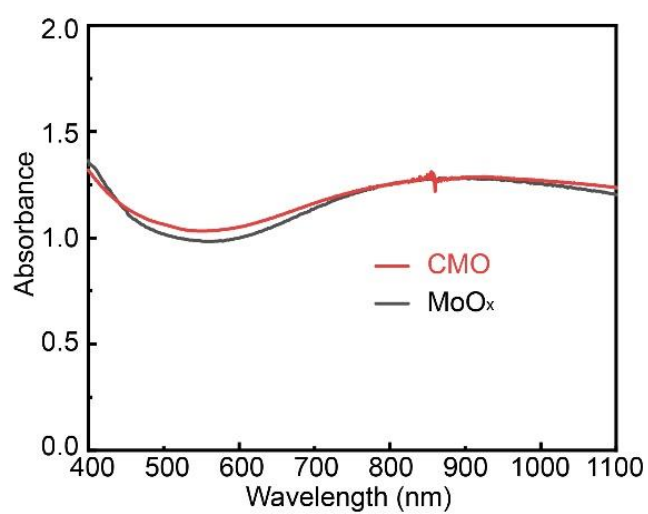


Figure S4. UV-Vis-NIR absorbance spectra of the CMO and MoO_x aqueous solution at the same particle concentration (200 ppm).

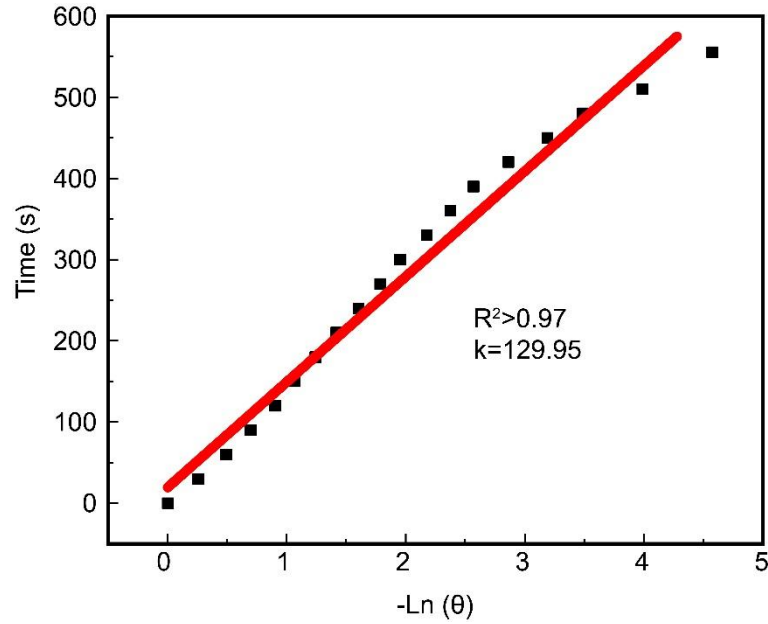


Figure S5. Fitting plots of time versus $-\ln \theta$ during the cooling period.

The photothermal conversion efficiency (η) indicates the performance of nanomaterials in converting the light into heat. The η value was calculated by the following equation (1):

$$\eta = \frac{hA(T_{max} - T_0) - Q_0}{I(1 - 10^{-A_\lambda})} \times 100\% \quad (1)$$

η : the photothermal conversion efficiency;

h (mV/(m² °C)): the heat-transfer coefficient;

A (m²): the container's surface area;

T_{max} (°C): laser-irradiated maximum temperature;

T_0 (°C): the initial temperature;

Q_0 (mW): the heat energy caused by the light absorbing of the solvent can be calculated by the process:

$$Q_0 = hA(T_{water,max} - T_0);$$

$T_{water,max}$ (°C): laser-irradiated maximum temperature for DI water;

I : the laser power;

A_λ : the absorbance of photothermal agent.

The value of hA can be calculated by the following equation (2):

$$hA = \frac{m_s c_s}{k} \quad (2)$$

m_s (g): the mass of the sample solution;

C_s (J/(g K)): the sample heat capacity.

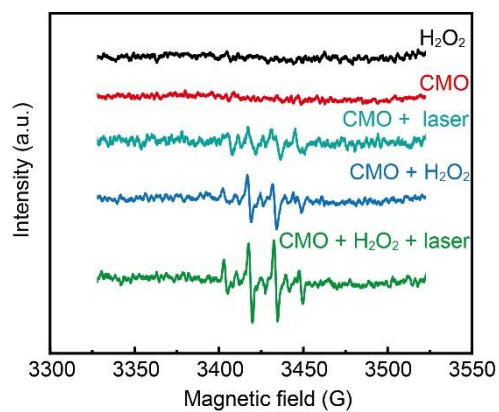


Figure S6. ESR spectra of different groups using DMPO as a trapping agent.

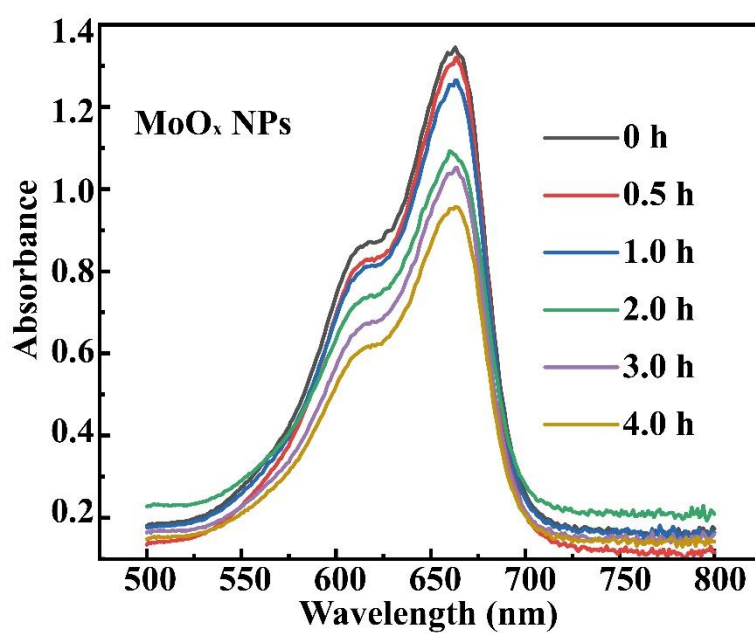


Figure S7. Degradation of MB in the MoO_x aqueous solution at different time points (0 h, 0.5 h, 1 h, 2 h, 3 h, 4 h).

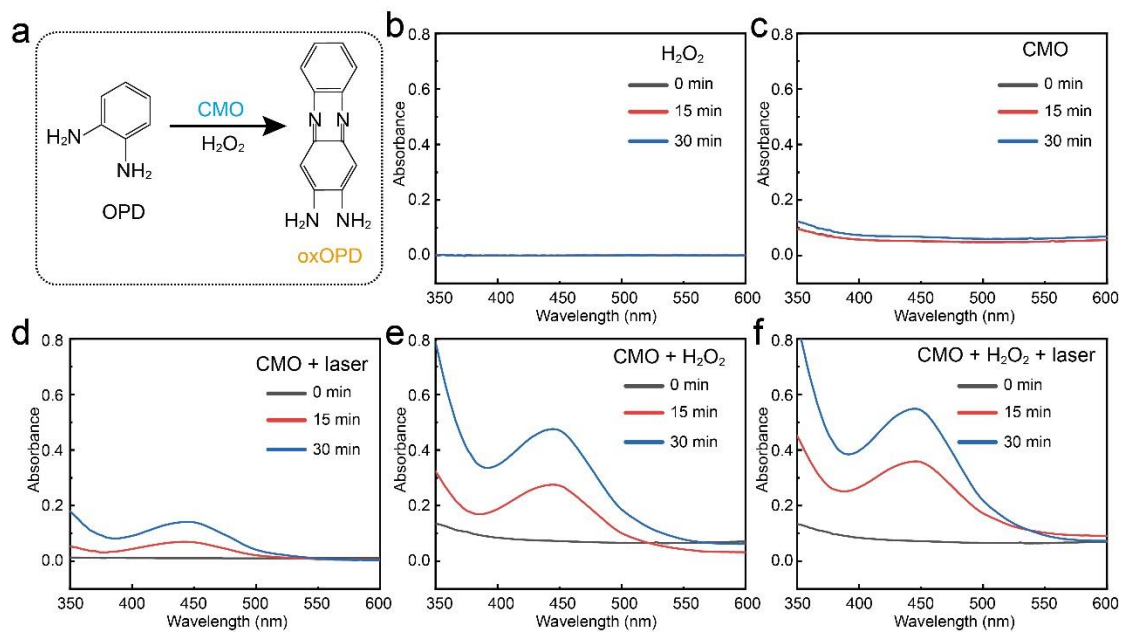


Figure S8. Detection of hydroxyl radicals with OPD. (a) Schematic illustration of the generation of $\cdot\text{OH}$ by CMO, UV-Vis absorption spectra of the following samples: (b) H₂O₂, (c) CMO, (d) CMO+laser, (e) CMO+H₂O₂, (f) CMO+H₂O₂+laser.

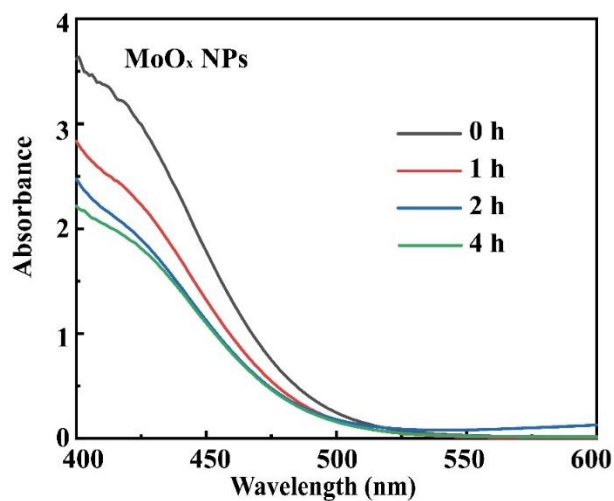


Figure S9. Changes of GSH consumption after oxidation with the MoO_x NPs at different time points (0 h, 1 h, 2 h, 4 h).

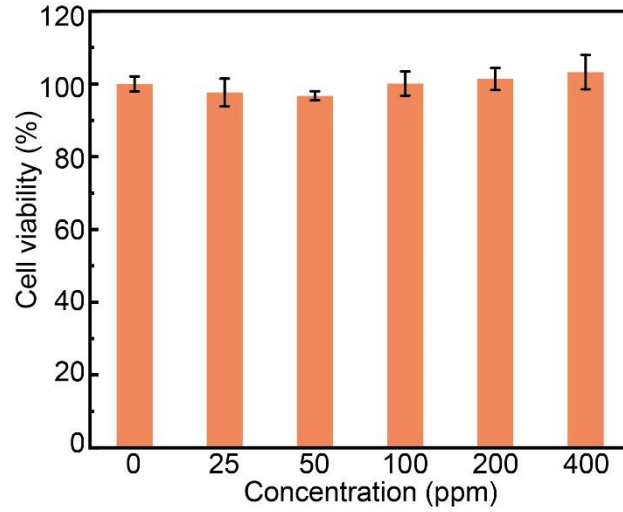


Figure S10. Cell viability of HAEC cells after 24 h of incubation with different concentrations of CMO.

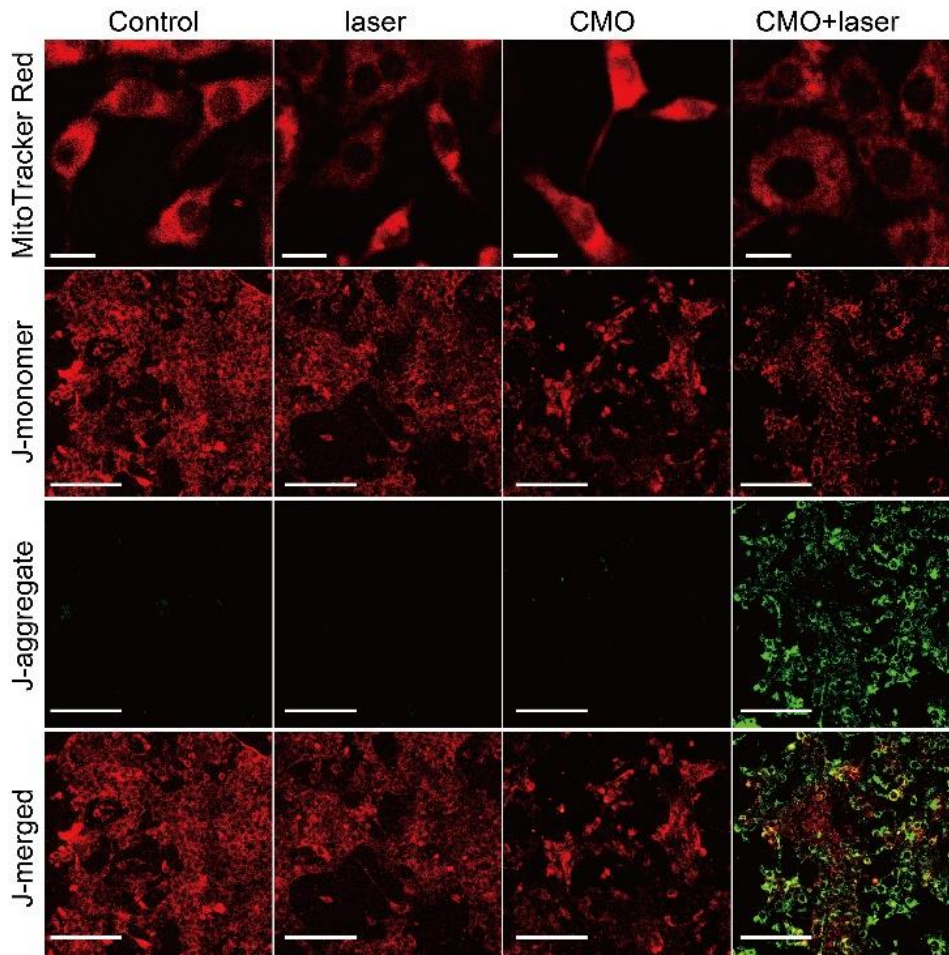


Figure S11. CLSM images of mitochondrial morphology (scale bar: 20 μm) in 4T1 cells after incubation with the CMO and effect of the CMO on mitochondrial membrane potential ($\Delta\psi\text{m}$) in 4T1 cells (scale bar: 200 μm).

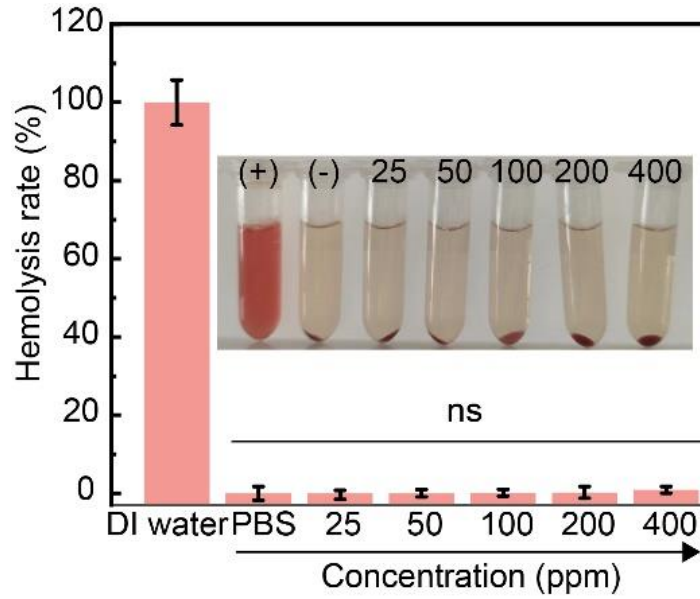


Figure S12. Hemolysis analysis of blood incubated with water (positive control) and different concentrations of CMO (inset is corresponding digital photograph).



Figure S13. Photographs of 4T1 tumor-bearing mice and their tumor regions after 14 days without and with laser treatments.

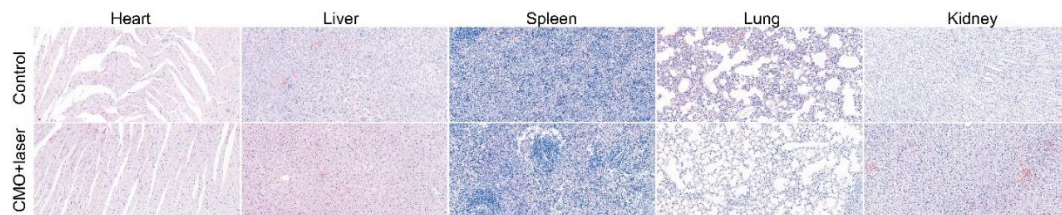


Figure S14. H&E-stained with major organs after 14 days for the Group I and VI mice.

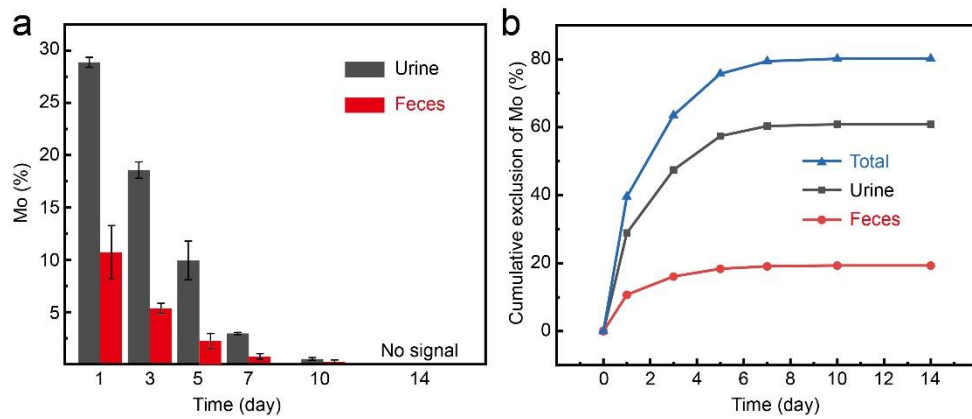


Figure S15. Metabolic study of CMO NPs. a) Mo% in urine and feces collected at various time points after injection and b) Cumulative exclusion of Mo%.